

Radicals induced from peroxomonosulfate by nanoscale zero-valent copper in the acidic solution

Peng Zhou, Bei Liu, Jing Zhang, Yongli Zhang, Gucheng Zhang, Chenmo Wei, Juan Liang, Ya Liu and Wei Zhang

ABSTRACT

A highly efficient advanced oxidation process for the degradation of benzoic acid (BA) during activation of peroxomonosulfate (PMS) by nanoscale zero-valent copper (nZVC) in acidic solution is reported. BA degradation was almost completely achieved after 10 min in the nZVC/PMS process at initial pH 3.0. PMS could accelerate the corrosion of nZVC in acidic to release Cu^+ which can further activate PMS to produce reactive radicals. Both sulfate radical ($\text{SO}_4^{\bullet-}$) and hydroxyl radical ($\bullet\text{OH}$) were considered as the primary reactive oxidant in the nZVC/PMS process with the experiments of methyl (MA) and *tert*-butyl alcohol quenching. Acidic condition (initial pH \leq 3.0) facilitated BA degradation and pH is a decisive factor to affect the oxidation capacity in the nZVC/PMS process. Moreover, BA degradation in the nZVC/PMS process followed the pseudo-first-order kinetics, and BA degradation efficiency increased with the increase of the nZVC dosage.

Key words | benzoic acid, hydroxyl radical, peroxomonosulfate, sulfate radical, zero-valent copper

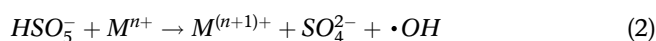
Peng Zhou
Bei Liu
Jing Zhang (corresponding author)
Yongli Zhang
Gucheng Zhang
Chenmo Wei
Juan Liang
Ya Liu
Wei Zhang
College of Architecture & Environment, Sichuan University,
Chengdu 610065, China
E-mail: zjing428@163.com

INTRODUCTION

Increasing attention has been paid to advanced oxidation processes (AOPs) resulting from the generation of reactive radicals (e.g. $\text{SO}_4^{\bullet-}$ and $\bullet\text{OH}$) (Duan *et al.* 2016; Peluffo *et al.* 2016) and its high efficiency on decomposing persistent organic pollutants. Among these AOPs, hydrogen peroxide (H_2O_2) (Chen *et al.* 2011), persulfate (PS) (Al-Shamsi & Thomson 2013), and peroxomonosulfate (PMS) (Zhou *et al.* 2015) are considered as inexpensive oxidants for the remediation of contaminated water resulting from these three common peroxides, precursors of $\text{SO}_4^{\bullet-}$ and $\bullet\text{OH}$. Recently, PMS has gained more attention from investigators because it is easily activated by transition metals, heat, ultraviolet, and ultrasound (Anipsitakis & Dionysiou 2004; Guan *et al.* 2011).

Many transition ions have been employed to activate PMS to produce reactive radicals (Equations (1)–(3)) resulting in the removal of organic contaminants, such as Fe(II), Fe(III), Co(II), Ru(III), Ag(I), Ce(III), V(III), Mn(II), and Ni(II) (Anipsitakis & Dionysiou 2004; Zou *et al.* 2013). However, Cu(I) was seldom used as an activator for PMS because Cu(I) is unstable and easily oxidized to Cu(II) by oxygen or other oxidants in aqueous solutions (Gonzalez-Davila *et al.* 2009), although Cu(I) could activate PS and H_2O_2 to induce

the generation of $\text{SO}_4^{\bullet-}$ and $\bullet\text{OH}$ (Kolthoff & Woods 1966; Masarwa *et al.* 1988; Zhou *et al.* 2016).



Currently, the corrosion of zero-valent metals in acidic solution could induce the *in situ* generation of H_2O_2 and intermediate low-valent metal ions which could further induce the generation of $\bullet\text{OH}$ by Fenton-like reaction (Joo *et al.* 2004; Bokare & Choi 2009). In addition, Wen and colleagues (Wen *et al.* 2014) reported that Cu^+ and H_2O_2 were formed in the zero-valent copper (ZVC) acidic system, which was due to the corrosive dissolution of ZVC and the concurrent reduction of oxygen, and $\bullet\text{OH}$ generated via the Fenton-like reaction of *in situ* generated Cu^+ with H_2O_2 was mainly responsible for the degradation of diethyl phthalate. Hence, nanoscale zero-valent copper (nZVC) is a potential zero-valent metal to generate Cu^+ during the

nZVC corrosion to activate PMS resulting in the generation of reactive radicals to degrade organic contaminants. As far as we know, nZVC has never been employed as an activator for PMS to degrade organic contaminants. Benzoic acid (BA) was selected as the radical probe compound in this study owing to the relatively simple structure and stable property with common oxidants but high rates constant with $\cdot\text{OH}$ (Buxton *et al.* 1988) and $\text{SO}_4\cdot^-$ (Neta *et al.* 1988).

The aim of this study is to investigate the degradation efficiency of BA in the nZVC/PMS process and to specifically focus on the mechanism of the nZVC/PMS process, identification of primary reactive oxidants, effect of initial pH, and effect of nZVC dosage.

MATERIALS AND METHODS

Materials

nZVC (size: 10–30 nm, >99.9%) and neocuproine hemihydrate (NCP, >98%) were of analytic purity and purchased from Aladdin Industrial Corporation. Oxone ($\text{KHSO}_5\cdot 0.5\text{KHSO}_4\cdot 0.5\text{K}_2\text{SO}_4$, PMS), copper sulfate pentahydrate ($\geq 99.0\%$), and BA ($\geq 99.5\%$) were of American Chemical Society (ACS) reagent grade and supplied by Sigma-Aldrich, Inc. Sodium sulfite, *tert*-butyl alcohol (TBA), sulfuric acid, and sodium hydroxide were of analytic purity and purchased from Sinopharm Chemical Reagent Co. Ltd, China. Methyl alcohol (MA) and ammonium acetate, which were purchased from Sigma-Aldrich, were of high performance liquid chromatography (HPLC) grade. Pure oxygen (O_2 , $\geq 99.2\%$) and pure nitrogen (N_2 , $\geq 99.99\%$) were stored in the special high-pressure gas cylinder.

Procedures

Experiments were performed in 500 mL under constant stirring with a polytetrafluoroethylene (PTFE)-coated magnetic stirrer at $10 \pm 0.5^\circ\text{C}$. Each 500 mL reaction solution with desired concentration of BA was prepared with ultrapure water and adjusted to desired initial pH with sulfuric acid and sodium hydroxide, and each run was switched on by adding the desired dosage of PMS and nZVC. Most of the experiments were operated open to the air. However, in order to investigate the effect of O_2 on the process, part of experiments were aerobic or anaerobic aqueous solutions through constant feeding of pure O_2 or N_2 . Desired TBA and MA were added into the reaction solution before the addition of PMS to identify the primary reactive radicals.

Moreover, NCP was used as Cu(I)-chelating to investigate the role of Cu^+ in the process. Samples were withdrawn at set intervals and quenched by sodium sulfite after filtration with glass fiber membrane of $0.45\ \mu\text{m}$ pore size.

Sample analysis

The concentration of BA was analyzed on HPLC (Waters e2695), equipped with 2489 λ absorbance detector (227 nm for BA) and reverse-phase C18 column ($4.6 \times 150\ \text{mm}$). The pH in aqueous solution was monitored by pH meter (Shanghai Leici Apparatus Fac., China). Total concentration of dissolved copper (TCu) were measured by a PerkinElmer[®] PinAAcle 900T flame atomic absorption spectrometer (Shelton, CT, USA) equipped with two hollow multi-element cathode lamps. Moreover, nZVC was characterized before and after reaction with X-ray diffraction (XRD, X'Pert Pro MPD diffractometer (Philips, The Netherlands)) and scanning electron microscopy (SEM, JSM-7500F (JEOL, Japan)).

RESULTS AND DISCUSSION

Degradation of BA in the nZVC/PMS process

Figure 1 shows the BA degradation in the PMS, Cu^{2+} /PMS, and nZVC/PMS processes at acidic solution (initial pH 3.0). Less than 2.0% BA was degraded after 10 min in the PMS process. Surprisingly, BA removal was completely achieved after 10 min in the nZVC/PMS process. Thus, the nZVC/PMS process is high-efficiency to degrade BA. In addition, only 3.0%

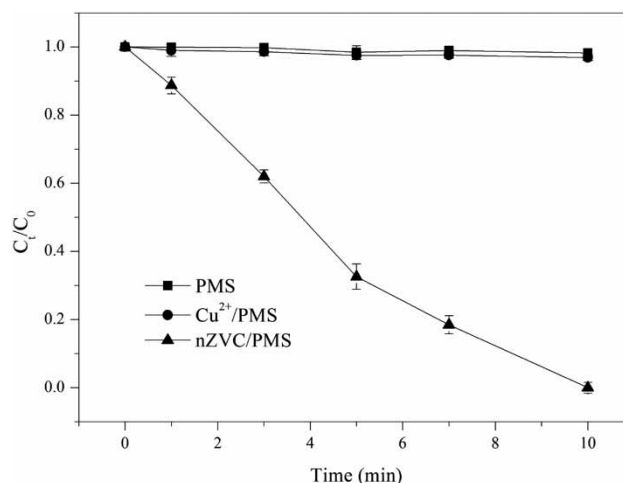


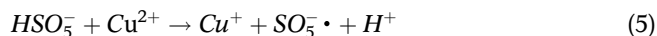
Figure 1 | Degradation of BA in the nZVC/PMS process. $[\text{BA}]_0 = 20\ \mu\text{M}$, $[\text{PMS}]_0 = 1\ \text{mM}$, $[\text{nZVC}]_0 = 40\ \text{mg/L}$, $[\text{Cu}^{2+}]_0 = 40\ \text{mg/L}$, $\text{pH}_0 = 3.0$.

BA was degraded in the Cu^{2+} /PMS process which shows that Cu^{2+} is not effective to activate PMS in acidic solution.

Effective copper species to activate PMS

Although Cu^+ has not been reported as an activator for PMS, Cu^+ can induce the generation of $\text{SO}_4^{\cdot-}$ and $\cdot\text{OH}$ via activating PS and H_2O_2 (Kolthoff & Woods 1966; Masarwa et al. 1988). Recently, Wen et al. (2014) reported that Cu^+ is a key intermediate during the corrosion of ZVC to induce the generation of $\cdot\text{OH}$ in the ZVC acidic system. Therefore, Cu^+ may be a potential intermediate to activate PMS during corrosion of nZVC in the nZVC/PMS process.

As an effective chelating agent for Cu^+ (Kim et al. 2015), less than 1.0% BA was degraded with the addition of 1 mM NCP after 10 min; by comparison, 10 μM BA was completely degraded after 10 min in the nZVC/PMS process. It could be inferred that Cu^+ is the main reactive copper species to activate PMS to produce $\text{SO}_4^{\cdot-}$ and $\cdot\text{OH}$ in the nZVC/PMS process via Equations (4)–(7) (Liang & Su 2009). Moreover, the direct activation of PMS by nZVC may be a possible way to induce the generation of reactive radicals. However, due to the total inhibition of BA degradation by adding NCP, the direct activation of PMS by nZVC should be a minor way.



Identification of reactive oxidants

It has been reported that $\text{SO}_4^{\cdot-}$, $\text{SO}_5^{\cdot-}$, and $\cdot\text{OH}$ could be produced for activation of PMS catalyzed by transition metals (Anipsitakis & Dionysiou 2004; Liang & Su 2009). All three reactive radicals may be formed in the nZVC/PMS process as shown in Equations (4)–(7). Resulting from the high rate constants with $\text{SO}_4^{\cdot-}$ ($k = 2.5 \times 10^7 \text{ M}^{-1}\text{s}^{-1}$) (Neta et al. 1988) and $\cdot\text{OH}$ ($k = 9.7 \times 10^8 \text{ M}^{-1}\text{s}^{-1}$) (Buxton et al. 1988), MA is an effective quencher for both $\text{SO}_4^{\cdot-}$ and $\cdot\text{OH}$. Owing to the high rate constant with $\cdot\text{OH}$ ($k = 6.0 \times 10^8 \text{ M}^{-1}\text{s}^{-1}$) (Buxton et al. 1988) and the much slower rate constant with $\text{SO}_4^{\cdot-}$ ($k = 8.0 \times 10^5 \text{ M}^{-1}\text{s}^{-1}$) (Neta et al. 1988), TBA is an effective quencher for $\cdot\text{OH}$ but not for $\text{SO}_4^{\cdot-}$. Simultaneously, $\text{SO}_5^{\cdot-}$ is

relatively inert toward MA and TBA with low rates (Hayon et al. 1972). On the basis of these properties, the quenching experiments with MA could allow us to differentiate the contribution between $\cdot\text{OH}/\text{SO}_4^{\cdot-}$ and $\text{SO}_5^{\cdot-}$, and the quenching experiments with TBA could allow us to differentiate the contribution between $\text{SO}_4^{\cdot-}$ and $\cdot\text{OH}$ on BA degradation.

As shown in Figure 2, the removal of BA was almost completely achieved in 10 min in the nZVC/PMS process. However, the removal of BA was almost completely inhibited with addition of 10 mM MA, which ruled out the contribution of $\text{SO}_5^{\cdot-}$ on BA degradation. Moreover, 37.5% BA was degraded in nZVC/PMS process with the addition of 10 mM TBA. Based on the comparison of the inhibition effect of MA and TBA on the removal of BA, it can be inferred that $\text{SO}_4^{\cdot-}$ and $\cdot\text{OH}$ were the primary reactive oxidants in the nZVC/PMS process.

Pathway of nZVC corrosion

As shown in Figure 3, nZVC was characterized by XRD before and after reaction. Results showed that the structure of nZVC before reaction was mainly composed by elementary Cu, whose three strongest lines corresponded to 2θ values of 43.2° , 50.2° , and 72.1° . Due to the relatively weak signal detection of the peaks at 35.3° , 38.7° , and 48.7° , it could be concluded that a little nZVC was oxidized to CuO. However, when reaction time came to 3 or 8 min, the peaks which refer to elementary Cu were significantly weakened, and the generation of $\text{Cu}(\text{OH})_2$ was proved by the detection of the minor peaks in the diffractograms. Moreover, Figure 4 shows the SEM images of nZVC before and after reaction in the

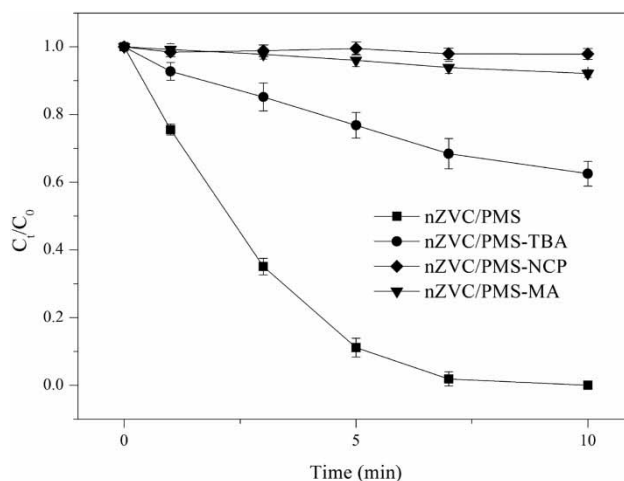


Figure 2 | Inhibition of NCP, MA, and TBA on BA degradation in nZVC/PMS process. $[\text{BA}]_0 = 20 \mu\text{M}$, $[\text{PMS}]_0 = 1 \text{ mM}$, $[\text{nZVC}]_0 = 40 \text{ mg/L}$, $[\text{MA}]_0 = [\text{TBA}]_0 = 10 \text{ mM}$, $[\text{NCP}]_0 = 1 \text{ mM}$, $\text{pH}_0 = 3.0$.

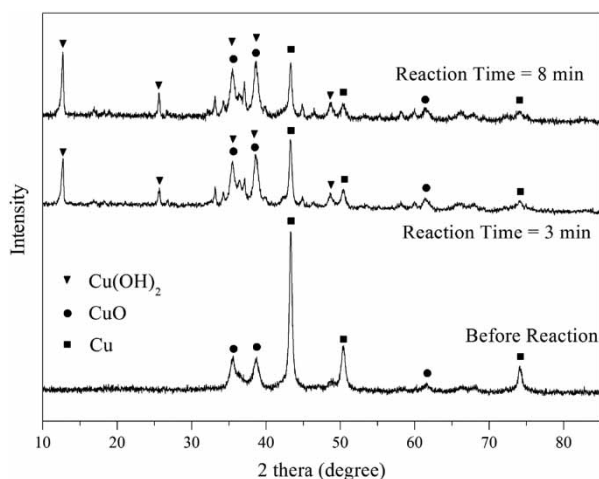
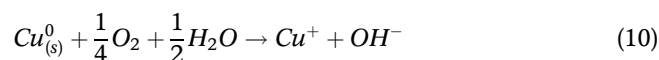
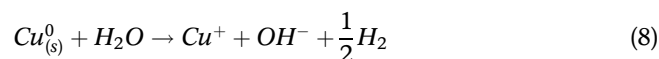


Figure 3 | Diffraction obtained in nZVC characterization by XRD before and after reaction in nZVC/PMS process.

nZVC/PMS process. It could be noted that nZVC was nano-sized spheroidal particle before reaction, and nZVC was gradually corroded resulting from the increase of the surface imperfection of nZVC as the reaction progressed in the nZVC/PMS process. A combination of XRD and SEM mapping analysis showed that nZVC was gradually dissolved into the reaction solution in the nZVC/PMS process.

Based on the results above, the pathway of Cu^+ release during nZVC corrosion is important in the nZVC/PMS

process because Cu^+ is the key intermediate to activate PMS. Similar to the corrosion of zero-valent iron, the Cu^+ release during nZVC corrosion may follow three possible pathways: (i) by deoxygenated water via Equation (8), (ii) by PMS via Equation (9), (iii) by dissolved oxygen (DO) via Equation (10). In order to investigate the pathway of Cu^+ release during nZVC corrosion, the variations of BA and dissolved TCu with reaction time were measured in aerobic (constant feeding O_2 , nZVC/PMS- O_2), anoxic (open to the air, nZVC/PMS), and anaerobic (constant feeding N_2 , nZVC/PMS- N_2) aqueous solutions at initial pH 3.0.



As shown in Figure 5(a) and 5(b), less than 4.0% BA was degraded with the addition of 40 mg/L nZVC in the nZVC acidic process. In previous literature (Wen *et al.* 2014), the ZVC acidic process was effective to degrade organic pollutants with the dosage of ZVC reached up to 0.5 g/L. Nevertheless, it is evident that the nZVC acidic system has low efficiency on BA

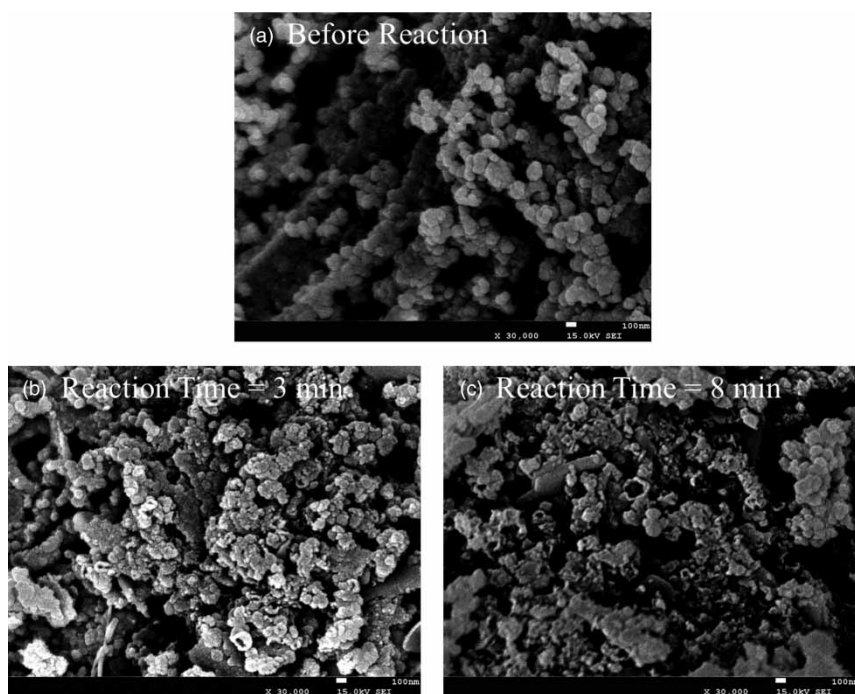


Figure 4 | SEM images of nZVC before (a) and after (b and c) reaction in nZVC/PMS process.

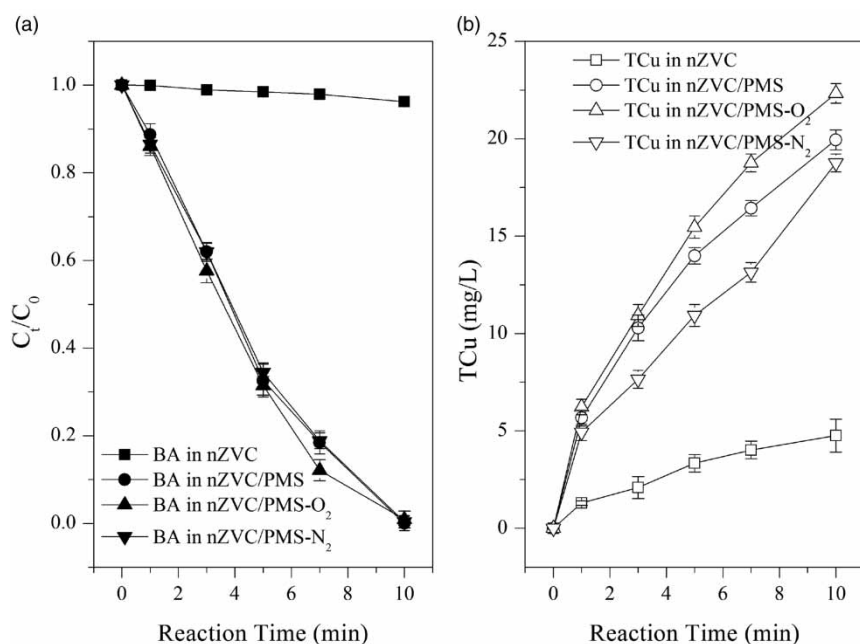


Figure 5 | Variations of BA (a) and TCu (b) with reaction time in the nZVC/PMS process under the aerobic, anoxic, and anaerobic solutions. [BA]₀ = 20 μM, [PMS]₀ = 1 mM, [nZVC]₀ = 40 mg/L, O₂ flow rate = 0.3 L/min, N₂ flow rate = 0.8 L/min, pH₀ = 3.0.

degradation with low dosage of nZVC and short reaction time. However, 18.8 mg/L nZVC was dissolved after 10 min resulting in the removal of BA was completely achieved in the nZVC/PMS-N₂ process. Based on strong enhancement of nZVC corrosion with the addition of PMS in anaerobic solution, it could be inferred that PMS can accelerate nZVC corrosion via Equation (9) to release Cu⁺ to activate PMS. Moreover, 19.9 and 22.3 mg/L TCu were respectively detected after 10 min in the nZVC/PMS and the nZVC/PMS-O₂ processes which shows that it is a slight pathway to dissolve nZVC via Equation (10). However, BA degradation has not been enhanced obviously in the nZVC/PMS and the nZVC/PMS-O₂ processes. Based on the results above, pathway (ii) is the primary pathway to dissolve nZVC, and DO is not indispensably essential for BA degradation in the nZVC/PMS process. The mechanism of the nZVC/PMS process is shown in Figure 6.

Effect of initial pH

Figure 7 shows the effect of initial pH on BA degradation in the nZVC/PMS process at the initial pH range of 2.0–5.8. BA was rapidly degraded at the initial pH range of 2.0–3.0, and lower pH facilitated the degradation of BA. For instance, the removal of BA was almost achieved after 10 min at initial pH 2.0, compared to only 25.5%, 11.0%, and 7.5% BA were respectively degraded at initial pH being 4.2, 4.8, and 5.8. In previous literature (Bokare & Choi 2009; Liu et al. 2011),

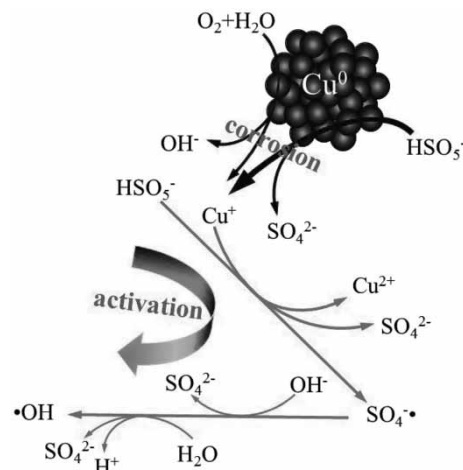


Figure 6 | The mechanism of the nZVC/PMS process.

H⁺ was prerequisite to dissolve the surface oxide layer before zero-valent aluminum corrosion. Thus, it was probably similar to zero-valent aluminum that H⁺ could accelerate the corrosion of nZVC's oxide layer in acidic solution to facilitate BA degradation in the nZVC/PMS process. Moreover, the higher pH may be conducive for OH⁻ to quench Cu⁺ because the decomposition of CuOH to form Cu₂O and H₂O is spontaneous in aqueous via Equations (11) and (12) (Li et al. 2015) which could inhibit the activation of PMS by Cu⁺. In summary, acidic condition (initial pH ≤ 3.0) facilitated BA degradation and pH is a decisive factor to affect the oxidation

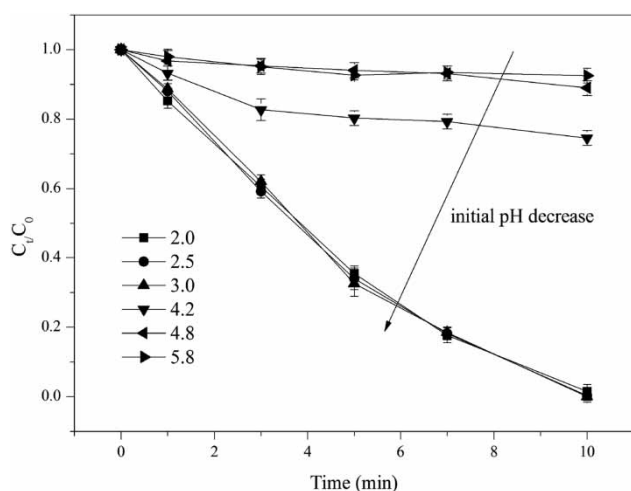


Figure 7 | Effect of initial pH on BA degradation in the nZVC/PMS process. $[BA]_0 = 20 \mu\text{M}$, $[PMS]_0 = 1 \text{ mM}$, $[nZVC]_0 = 40 \text{ mg/L}$, $\text{pH}_0 = 2.0, 2.5, 3.0, 4.2, 4.8, \text{ and } 5.8$.

capacity in the nZVC/PMS process.



Effect of nZVC dosage

The nZVC dosage may be a crucial factor for BA degradation in the nZVC/PMS process. Figure 8 shows the effect of nZVC dosage on BA degradation in the nZVC/PMS process at initial

pH 3.0. The BA removal efficiency increased gradually as the dosage of nZVC increased from 5 to 60 mg/L. For example, the degradation of BA after 10 min increased from 23.1% with 5 mg/L to ~100% with 60 mg/L. Moreover, BA degradation fit well with the pseudo-first-order kinetics, and BA degradation rates were respectively 0.023 ($R^2 = 0.95$), 0.042 ($R^2 = 0.99$), 0.109 ($R^2 = 0.92$), 0.155 ($R^2 = 0.96$), 0.226 ($R^2 = 0.96$), and 0.355 ($R^2 = 0.95$) min^{-1} with the nZVC dosage being 5, 10, 20, 30, 40, and 60 mg/L. The enhancement of Cu^+ release which could enhance the activation of PMS to produce $\text{SO}_4^{\cdot-}$ and $\cdot\text{OH}$ with an increase of nZVC dosage is likely responsible for the increase of BA degradation rate.

CONCLUSION

This study investigated the activation of PMS by nZVC and set up the nZVC/PMS process to effectively degrade BA in acidic aqueous solution. BA was almost completely degraded after 10 min, and BA degradation fit well with pseudo-first-order kinetics in the nZVC/PMS process at initial pH 3.0. PMS can accelerate the corrosion of nZVC to release Cu^+ resulting in further activation of PMS via the Fenton-like reaction to produce reactive radicals, and Cu^+ is the main active copper species to activate PMS at acidic solution. Due to the partial or almost complete inhibition of BA degradation with the addition of MA or TBA, both $\text{SO}_4^{\cdot-}$ and $\cdot\text{OH}$ were considered as the primary reactive oxidants in the nZVC/PMS process. Moreover, pH is a

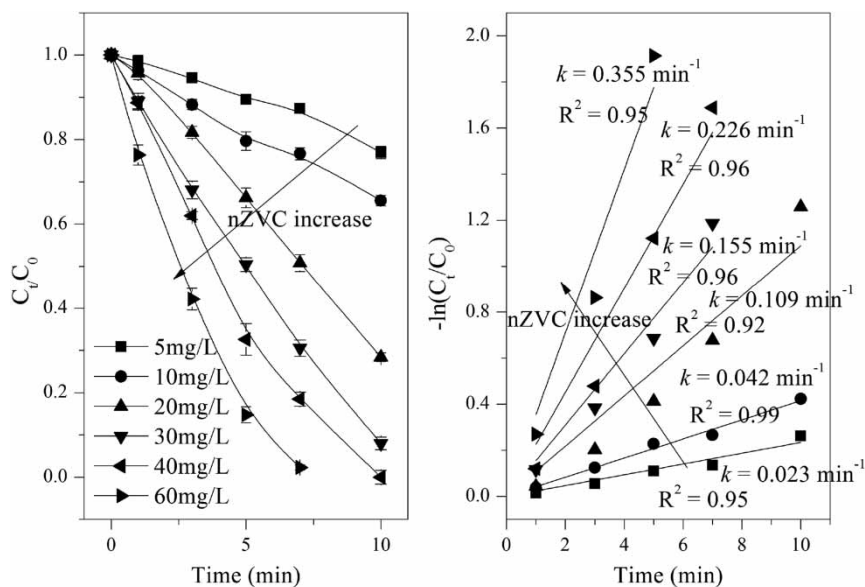


Figure 8 | Effect of nZVC dosage on BA degradation in the nZVC/PMS process. $[BA]_0 = 20 \mu\text{M}$, $[PMS]_0 = 1 \text{ mM}$, $[nZVC]_0 = 5, 10, 20, 30, 40, \text{ and } 60 \text{ mg/L}$, $\text{pH}_0 = 3.0$.

decisive factor to affect the oxidation capacity and acidic condition (initial $\text{pH} \leq 3.0$) facilitated BA degradation in the nZVC/PMS process. BA degradation efficiency increased with the increase of nZVC dosage. In addition, the nZVC/PMS process overcame the drawback of instability of Cu^+ and put forward an interesting idea to make full use of intermediate Cu^+ to activate active oxidants during the corrosion of nZVC to degrade organic pollutants.

ACKNOWLEDGEMENTS

Appreciation and acknowledgment are given to the National Natural Science Foundation of China (No. 51508353) and the National Natural Science Foundation of China (No. 51408349).

REFERENCES

- Al-Shamsi, M. A. & Thomson, N. R. 2013 Treatment of organic compounds by activated persulfate using nanoscale zerovalent iron. *Industrial & Engineering Chemistry Research* **52** (38), 13564–13571.
- Anipsitakis, G. P. & Dionysiou, D. D. 2004 Radical generation by the interaction of transition metals with common oxidants. *Environmental Science & Technology* **38** (13), 3705–3712.
- Bokare, A. D. & Choi, W. 2009 Zero-valent aluminum for oxidative degradation of aqueous organic pollutants. *Environmental Science & Technology* **43** (18), 7130–7135.
- Buxton, G. V., Greenstock, C. L., Helman, W. P. & Ross, A. B. 1988 Critical-review of rate constants for reactions of hydrated electrons, hydrogen-atoms and hydroxyl radicals ($\cdot\text{OH}/\cdot\text{O}$) in aqueous-solution. *Journal of Physical and Chemical Reference Data* **17** (2), 513–886.
- Chen, L. W., Ma, J., Li, X. C., Zhang, J., Fang, J. Y., Guan, Y. H. & Xie, P. C. 2011 Strong enhancement on Fenton oxidation by addition of hydroxylamine to accelerate the ferric and ferrous iron cycles. *Environmental Science & Technology* **45** (9), 3925–3930.
- Duan, X., Su, C., Zhou, L., Sun, H., Suvorova, A., Odedairo, T., Zhu, Z., Shao, Z. & Wang, S. 2016 Surface controlled generation of reactive radicals from persulfate by carbocatalysis on nanodiamonds. *Applied Catalysis B: Environmental* **194**, 7–15.
- Gonzalez-Davila, M., Santana-Casiano, J. M., Gonzalez, A. G., Perez, N. & Millero, F. J. 2009 Oxidation of copper(I) in seawater at nanomolar levels. *Marine Chemistry* **115** (1–2), 118–124.
- Guan, Y. H., Ma, J., Li, X. C., Fang, J. Y. & Chen, L. W. 2011 Influence of pH on the formation of sulfate and hydroxyl radicals in the UV/peroxymonosulfate system. *Environmental Science & Technology* **45** (21), 9308–9314.
- Hayon, E., Treinin, A. & Wilf, J. 1972 Electronic-spectra, photochemistry, and autoxidation mechanism of sulfite-bisulfite-pyrosulfite systems SO_2^- , SO_3^- , SO_4^- , and SO_5^- radicals. *Journal of the American Chemical Society* **94** (1), 47–57.
- Joo, S. H., Feitz, A. J. & Waite, T. D. 2004 Oxidative degradation of the carbothioate herbicide, molinate, using nanoscale zero-valent iron. *Environmental Science & Technology* **38** (7), 2242–2247.
- Kim, H. E., Nguyen, T. T. M., Lee, H. & Lee, C. 2015 Enhanced inactivation of *Escherichia coli* and MS2 coliphage by cupric ion in the presence of hydroxylamine: dual microbicidal effects. *Environmental Science & Technology* **49** (24), 14416–14423.
- Kolthoff, I. M. & Woods, R. 1966 Polarographic kinetic currents in mixtures of persulfate and copper (II) in chloride medium. *Journal of the American Chemical Society* **88** (7), 1371–1375.
- Li, Y. G., Lousada, C. M., Soroka, I. L. & Korzhavyi, P. A. 2015 Bond network topology and antiferroelectric order in cupric CuOH. *Inorganic Chemistry* **54** (18), 8969–8977.
- Liang, C. J. & Su, H. W. 2009 Identification of sulfate and hydroxyl radicals in thermally activated persulfate. *Industrial & Engineering Chemistry Research* **48** (11), 5558–5562.
- Liu, W. P., Zhang, H. H., Cao, B. P., Lin, K. D. & Gan, J. 2011 Oxidative removal of bisphenol A using zero valent aluminum-acid system. *Water Research* **45** (4), 1872–1878.
- Masarwa, M., Cohen, H., Meyerstein, D., Hickman, D. L., Bakac, A. & Espenson, J. H. 1988 Reactions of low-valent transition-metal complexes with hydrogen-peroxide. Are they Fenton-like or not? 1. The case of Cu_{Aq}^+ and $\text{Cr}_{\text{Aq}}^{2+}$. *Journal of the American Chemical Society* **110** (13), 4293–4297.
- Neta, P., Huie, R. E. & Ross, A. B. 1988 Rate constants for reactions of inorganic radicals in aqueous-solution. *Journal of Physical and Chemical Reference Data* **17** (3), 1027–1284.
- Peluffo, M., Pardo, F., Santos, A. & Romero, A. 2016 Use of different kinds of persulfate activation with iron for the remediation of a PAH-contaminated soil. *Science of the Total Environment* **563–564**, 649–656.
- Wen, G., Wang, S. J., Ma, J., Huang, T. L., Liu, Z. Q., Zhao, L. & Xu, J. L. 2014 Oxidative degradation of organic pollutants in aqueous solution using zero valent copper under aerobic atmosphere condition. *Journal of Hazardous Materials* **275**, 193–199.
- Zou, J., Ma, J., Chen, L. W., Li, X. C., Guan, Y. H., Xie, P. C. & Pan, C. 2013 Rapid acceleration of ferrous iron/peroxymonosulfate oxidation of organic pollutants by promoting Fe(III)/Fe(II) cycle with hydroxylamine. *Environmental Science & Technology* **47** (20), 11685–11691.
- Zhou, P., Zhang, J., Liang, J., Zhang, Y., Liu, Y. & Liu, B. 2016 Activation of persulfate/copper by hydroxylamine via accelerating the cupric/cuprous redox couple. *Water Science & Technology* **73** (3), 493–500.
- Zhou, Y., Jiang, J., Gao, Y., Ma, J., Pang, S. Y., Li, J., Lu, X. T. & Yuan, L. P. 2015 Activation of peroxymonosulfate by benzoquinone: a novel nonradical oxidation process. *Environmental Science & Technology* **49** (21), 12941–12950.